Microstructure and deformation mechanisms of a solid propellant using 1H NMR spectroscopy

Aurélie Azoug, Andrei Constantinescu, Robert Nevière, Guy Jacob

Microstructure and deformation mechanisms of a solid propellant using ^{1}H NMR spectroscopy

Aurélie Azoug [a,*], Andrei Constantinescu [a], Robert Nevière [b], Guy Jacob [b]

[a] *Laboratoire de Mécanique des Solides – CNRS UMR 7649, Ecole Polytechnique, 91128 Palaiseau, France*
[b] *Herakles, Centre de Recherches du Bouchet, 9 Rue Lavoisier, 91710 Vert-le-Petit, France*

Highly-filled elastomers such as solid propellants exhibit a complex nonlinear viscoelastic behavior. The microstructural origin of this behavior is difficult to ascertain with macroscopic observations. This article aims at identifying the deformation mechanisms of a solid propellant by measuring the change in segmental mobility with deformation. The novelty lies in the use of ^{1}H Nuclear Magnetic Resonance (NMR) spectrometry to investigate the spin–spin relaxation times T_2 of a solid propellant. In addition, the effect of strain on T_2 is measured using a specific setup transmitting the loading of the tensile machine to the sample inside the NMR apparatus. We compare isolated components, unfilled binders, and solid propellants varying in composition according to a design of experiments. The design of experiments determines the influences of the filler fraction, the amount of curing agents, the plasticizer content, and the presence of filler–binder bonding agents, on the segmental mobilities. The propellant protons can be schematically divided into three segmental mobilities corresponding to distinct relaxation times. The short times correspond to the severely restricted segments situated around cross-links or fillers. The intermediate relaxation times correspond to segments of polymer chains linked at both ends. Finally, the long relaxation times correspond to the highly mobile segments of polymers (dangling ends) and to the plasticizer molecules. The influence of strain on the relaxation times shows that the polymer network is stretched between the fillers while part of the polymer in the sol fraction is immobilized. In addition, chain sliding on the filler surface and breaking of filler–binder links can occur.

* Corresponding author at: Johns Hopkins University, Department of Mechanical Engineering, 3400N. Charles st., Baltimore, MD 21218, USA. Tel.: +1 (510)847 8511.
E-mail address: aurelie.azoug@polytechnique.edu (A. Azoug).

1. Introduction

Solid propellants are highly-filled elastomers, used for the propulsion of rocket launchers. The main physical characteristic of this class of materials is the large filler fraction, up to 88%wt or 80% in volume, immersed in an elastomeric binder. Moreover, the binder in solid propellants is not fully cross-linked and incorporates a large quantity of plasticizer molecules. Consequently, the binder contains a significant amount of sol fraction, that is the fraction of the binder that can be extracted by swelling. The sol fraction is constituted of polymer chains and plasticizer and participate actively in the nonlinearity of the mechanical behavior [1–3]. Schematically, the propellant is composed of the fillers, the polymer network, and the sol fraction. The polymer network and the sol fraction constitute the binder.

The relations between the nonlinear mechanical behavior at the macroscopic scale and the microstructure at the scale of the fillers or the polymer chains have been explored [1–6]. However, direct experimental evidence of the physical mechanisms of deformation at the scale of the polymer network is difficult to obtain. In order to reach this goal, we precisely explore the deformation mechanisms in the binder of solid propellants by measuring the change in segmental mobility with deformation using nuclear magnetic spectrometry. The novelty of the approach lies in the application of this method to measure and understand the influence of strain on the segmental mobility. For solid propellants, this type of measurement has only been performed on an isolated binder in [7].

The ^{1}H Nuclear Magnetic Resonance (NMR) T_2 relaxometry directly measures the transversal spin relaxation of the protons of the polymer chain, without modifications of or additions to the material under scrutiny [8,9]. The spin relaxation takes place at an atomic scale and is influenced by the local environment of each proton [10]. As a consequence, the transversal or spin–spin relaxation time T_2 of the spins varies according to the mobility of the molecular segment on which they are situated. Therefore, the ^{1}H NMR T_2 relaxometry enables the measure of segmental mobility [9]. The measurement commonly results in the continuous spectrum of relaxation times for the protons in the material. If the material is considered to be heterogeneous [11], i.e. made of different type of segments or phases, then commonly the continuous spectrum is discretized in a series of different systems each associated with segments. The corresponding discrete relaxation times are then the average time of each mobility. The relative contribution of each segment type to the total relaxation spectrum is proportional to the quantity of protons on these types of segments [10].

Previous investigations of filled and unfilled elastomers showed that the introduction of fillers creates a microstructure containing a large range of segmental mobility [12–18]. The segments of the polymer network in the bulk of the binder present a higher mobility than the segments close to the fillers but an overall lower mobility than the same unfilled elastomer [12–14,19,20]. Topological constraints created by the fillers reduce the mobility of all the polymer segments [15]. In the case of reinforcing fillers, a highly-constrained phase is measured and corresponds to immobilized polymer segments on the surface of the fillers [10]. Finally, free polymer molecules participate in the high mobility fraction [17].

The influence of deformation on segmental dynamics has been explored through T_2 relaxometry experiments on strained unfilled and filled elastomers [21–26]. The overall conclusion of the studies is that an increasing tensile strain emphasizes the anisotropy of the network causing a decrease of the relaxation time [27–31]. In addition, the sol fraction interact with network chains and orient according to network deformation [32–34].

2. Materials and methods

2.1. Materials

Three categories of materials have been tested: (i) hydroxyl-terminated polybutadiene (HTPB) polymer chains and plasticizer molecules, to allow the comparison with other systems, (ii) two binders corresponding to an HTPB polymer network, without and with plasticizers, denoted as 1 and 2, respectively, and (iii) a large number of propellant systems.

The propellant systems have as fillers ammonium perchlorate and aluminum, with sizes 20–200 μm and 5 μm, respectively. Filler–binder bonding agents (FBBA) are introduced to prevent or delay dewetting by linking chemically to the polymer chains in the binder and to the filler surface [35]. The exact synthesis of the FBBA molecules is confidential and will therefore not be described. More details on the FBBA are provided in [6] but are not essential to this study.

The binder is constituted of HTPB prepolymer cured with a methylene diicyclohexyl isocyanate (MDCI). The ratio of the quantity of isocyanate functions NCO with respect to the quantity of hydroxyl functions OH in the introduced polymer determines the NCO/OH ratio. In short, the NCO/OH ratio is a measure of the relative quantity of curing agents. The plasticizer introduced is dioctyl azelate (DOZ) molecules.

The materials are thermally cured for 2 weeks at 50 °C. The propellants numbered 0 to 21 (Table 1) correspond to a design of experiment (DoE) allowing us to determine the influence of four composition factors (the filler fraction, the FBBA, the NCO/OH ratio, and the plasticizer content) on the properties of an HTPB-based solid propellant. The principles of building the DoE have been detailed elsewhere [1,6].

2.2. ^{1}H NMR spectroscopy

2.2.1. CPMG sequence

All ^{1}H NMR T_2 relaxation measurements were conducted in the solid at room temperature, *i.e.* above the glass transition of all the tested materials, using a low resolution DIASPEC apparatus (ARTEC systems, frequency 19.623 MHz). The pulse sequence employed for the relaxation experiments was the standard Hahn-echo or CPMG [36,37] two pulse sequence conducted on resonance $90\,\mathrm{deg} - [\tau - 180\,\mathrm{deg} - \tau]_n - echo$. The CPMG sequence does not avoid the "dead time" of the NMR spectrometer, in this case 20 μs, and thus, focuses on the relatively long relaxation times [10]. The protons of the material with a very low mobility such as those in the fillers are not measured. The length of the 90 and 180 pulse is 7.5 and 15 μs, respectively. τ is equal to 55 μs and n is chosen between 700 and 1000 to observe the full decay. Finally, to limit the influence of the noise, the sequence is repeated between 32 and 64 times at time intervals of 1 s.

2.2.2. Strained NMR setup

To study the influence of mechanical deformation on the segmental mobility of the propellant, a setup combining the NMR apparatus and an INSTRON tensile machine is developed. The NMR apparatus is placed on the base of the tensile machine (Fig. 1(a)). The stresses are transmitted through a frame made of steel for the exterior parts and PEEK (PolyEtherEtherKetone) for the interior parts (Fig. 1). This polymer has no influence on the NMR results because its protons exhibit a very low mobility [38]. In addition, PEEK provides a high mechanical strength to the set up. Several teams have built similar setups dedicated to NMR spectrometry of strained specimens [21,28,38–41].

Table 1
Description of the tested materials. Presence or absence of FBBA is denoted by y (yes) and n (no), respectively.

	Mat.	Fillers (%wt)	FBBA	NCO/OH ratio	Plasticizer (%wt of the binder)	Sol polymer (%wt of the binder)
Molecules	HTPB	0	–	n	0.0	100.0
	DOZ	0	–	n	100.0	0.0
Binders	1	0	n	unknown	0.0	0.0
	2	0	n	unknown	16.0	19.4
Propellants	Ref.	88	y	0.8	22.5	26.7
	0	86	n	1.1	10.0	15.0
	1	90	n	0.8	30.0	63.0
	2	86	y	1.1	20.0	4.3
	3	90	y	0.8	20.0	46.0
	4	86	n	1.1	30.0	4.3
	5	90	y	1.1	30.0	5.0
	6	90	n	0.8	10.0	44.0
	7	86	y	0.8	10.0	37.9
	8	86	n	0.8	20.0	43.6
	9	86	y	0.8	30.0	42.1
	10	90	n	0.95	20.0	25.0
	11	88	n	1.1	20.0	13.3
	12	90	y	1.1	10.0	12.0
	13	88	y	0.95	30.0	13.3
	14	88	y	0.95	15.0	17.5
	15	88	n	0.88	25.0	29.2
	16	88	n	0.95	10.0	23.3
	17	90	y	0.8	10.0	47.0
	18	86	n	0.8	10.0	45.7
	19	86	y	1.1	10.0	7.9
	20	89	n	1.1	20.0	11.8
	21	89	n	0.8	10.0	46.4

For each material, a rectangular specimen of dimensions $50 \times 10 \times 5$ mm is glued to PEEK grips, placed in the NMR apparatus and fastened using the PEEK grips to the tensile machine. The detection coil in the apparatus exhibits a height of 20 mm, which determines the measurement window. The mechanical strain, applied at a strain rate of 0.1%/s, reaches up to 20%, the maximal value depending on the elongation at failure of each material. If the maximum elongation is lower than 8%, the specimen is tested every 1% of strain, otherwise, every 2% of strain. As a precaution, in order to reach a mechanical quasi-equilibrium state, the specimen is left to relax between 5 and 30 min before measuring the segmental mobility.

2.2.3. Signal processing

The NMR test provides the echo height $M(t)$ as a function of time t. Because the material quantity seen by the NMR apparatus varies during stretching – one part will exit the observation window (Fig. 1), the height of the echo is normalized so that the quantity of material in the apparatus does not influence the results. Accordingly, the materials can be quantitatively compared to each other.

This raw data is deconvoluted by an inverse Laplace transform:

$$\frac{M(t)}{M(0)} = \sum_{i=1}^{80} A_i \exp\left(-\frac{t}{T_{2i}}\right), \tag{1}$$

where $M(0)$ is the height of the echo at the time $t = 0$, T_{2i} the discretized spectrum of the relaxation times T_2, and A_i the amplitude associated with each T_{2i}. An example of the result can be seen in Fig. 2.

This discretized spectrum makes it uneasy to quantitatively compare the materials of the DoE, which is necessary to determine the influence of each factor. From this first processing, we chose to represent the behavior of the propellants with 3 relaxation times. The relaxation times T_2 and the associated fractions of the material f are determined from the normalized echo height $M(t)/M(0)$ using Eq. (2).

$$\frac{M(t)}{M(0)} = f_s e^{\left(-\frac{t}{T_{2s}}\right)} + f_m e^{\left(-\frac{t}{T_{2m}}\right)} \cdots + f_l e^{\left(-\frac{t}{T_{2l}}\right)}, \tag{2}$$

where s, m, and l stand for short, medium, and long, respectively, and $f_s + f_m + f_l = 1$. The parameters f_s, f_m, f_l, T_{2s}, T_{2m}, and T_{2l} have been identified from the NMR measurements using a Levenberg–Marquardt algorithm in Mathematica®. An example of the raw signal and its decomposition into three exponential terms is presented in Fig. 3. A correlation coefficient higher than 0.96 is obtained for all the fitted data.

In order to quantify the effective mechanical strain imposed to the specimen, we assume incompressibility and the rough approximation of the Gaussian network theory [42]. As a consequence, the effective strain λ^* is defined as:

$$\lambda^* = \lambda^2 - \frac{1}{\lambda} \tag{3}$$

where λ is the imposed tensile stretch. In the studied range, λ^* is proportional to λ. The use of this variable allows to take into account the effect of large deformations and to compare with previous studies [21,28,40]. We note that λ^* does not represent the effective strain at the molecular scale, which would depend on multiple factors and most prominently on strain amplification.

The influence of the effective strain on the relaxation times T_{2i} and associated fractions f_i is quantified by $\partial T_{2i}/\partial\lambda^*$ and $\partial f_i/\partial\lambda^*$, respectively (Fig. 4).

2.3. DoE analysis

Finally, as presented in details in [1,6], the DoE method is applied to the 12 responses: T_{2s}, T_{2m}, T_{2l}, f_s, f_m, f_l, and their derivatives with respect to the effective strain λ^*, $\partial T_{2s,\lambda^*}$, $\partial T_{2m,\lambda^*}$, $\partial T_{2l,\lambda^*}$, $\partial f_{s,\lambda^*}$, $\partial f_{m,\lambda^*}$, and $\partial f_{l,\lambda^*}$, using the Design-Expert® software. A model with n coefficients can only be investigated with a DoE consisting of at least n runs. According to the number of factors chosen and the number of materials manufactured, the possible models are: mean value, linear, first order interactions,

(a) Picture of the stretched NMR set up

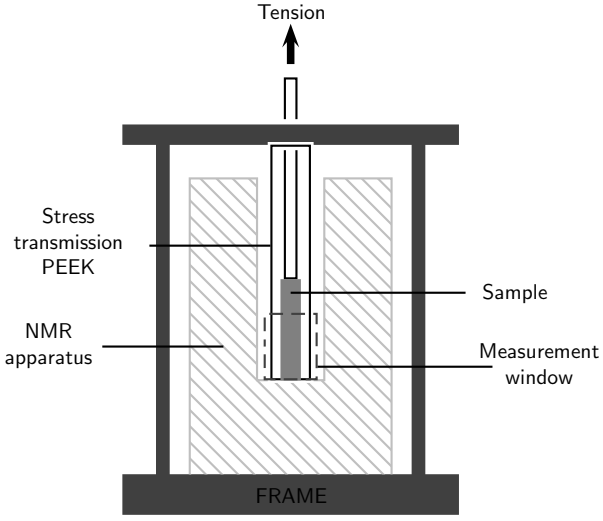

(b) Scheme of the stretched NMR set up

Fig. 1. NMR set up in the tensile machine.

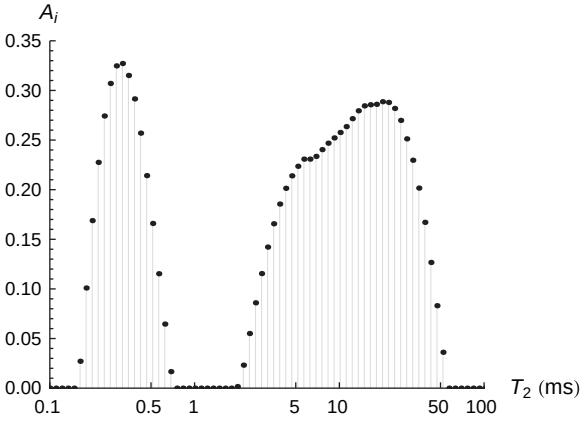

Fig. 2. Example of the inverse Laplace transform applied to the magnetization decay of the propellant 'Ref'.

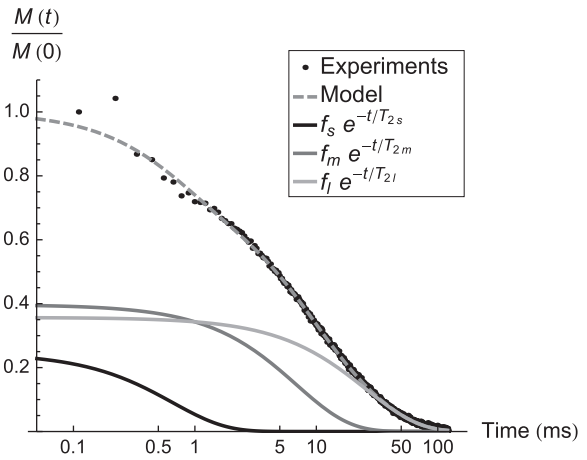

Fig. 3. Magnetization decay of the propellant 'Ref' and its decomposition according to Eq. (2).

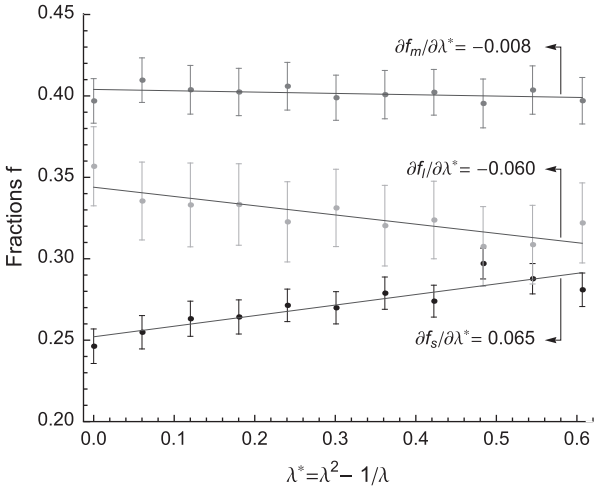

(a) Fractions f

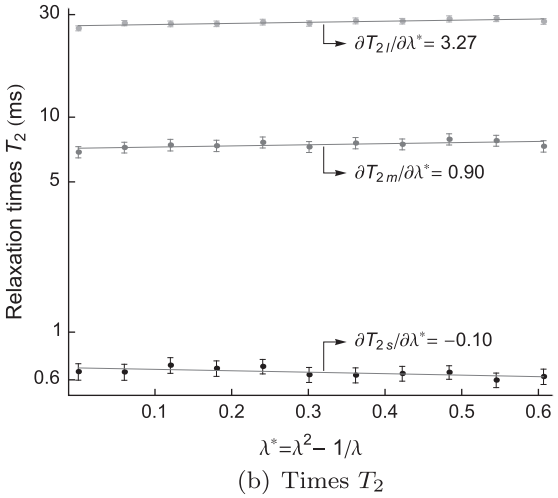

(b) Times T_2

Fig. 4. Relaxation times and fractions of the propellant 'Ref' according to strain.

or quadratic. The unknowns constants of the model are obtained by optimization on the experimental results. An analysis of variance determines the model form best representing the results while taking into account the least number of terms. A second analysis

of variance is performed on the chosen model form to eliminate the terms corresponding to non influential factors or interactions (p-value < 0.05).

The final model represents the response according to the factors of the DoE, here variables of material composition. The good fit of the model is evaluated by the adjusted correlation coefficient R^2_{adj} [43], which takes into account the number of terms in the model.

3. Results and discussion

3.1. Fit of the DoE models

Table 2 specifies the R^2_{adj} for each parameter p and its derivative with respect to the effective strain $\partial p_{,\lambda^*} = \partial p/\partial \lambda^*$.

The $R^2_{adj}(\partial p_{,\lambda^*})$ are, as expected, lower than $R^2_{adj}(p)$. However, only $R^2_{adj}(\partial f_{s,\lambda^*})$ and $R^2_{adj}(\partial T_{2m,\lambda^*})$ show that the obtained models unsatisfyingly fit the experimental data. The lack of fit originates from two factors. First, the derivatives are of the order of 10^{-2} for the fractions f_i and of the order of 10^{-1} or 1 for the times T_{2i}. The influence of noise on the experimental data is then statistically significant during the DoE processing. Second, the used CPMG sequence focuses on the relatively long relaxation times. As the material is stretched, the protons in the low mobility segments become even more constrained and their relaxation time might become too short to be measured with this sequence. The low correlation between the slope of f_s and the model results from this technical limit.

3.2. Relaxation of the microstructure

In short, the microstructure of a solid propellant can be schematically decomposed into the fillers, the polymer network and the sol fraction, which contains the sol polymer and plasticizer molecules [6,1].

3.2.1. The fillers

Fig. 5 compares the relaxation times of the HTPB molecules, the plasticizer molecules, binder 1, binder 2, and a solid propellant. The comparison of binder 2 and the propellant 'Ref' shows that introducing fillers leads to a decrease of .3 and 16 ms of the times T_{2s} and T_{2l}, i.e. 30.6% and 37.9% respectively. T_{2m} remains constant.

The DoE provides further information on the influence of the filler fraction on the relaxation times (Fig. 6) and their associated fractions. The DoE models indicate that the filler fraction has no influence on the fractions f_s, f_m, and f_l. Again, T_{2s} decreases while T_{2m} remains constant with an increase in filler fraction. According to the DoE models, T_{2l} does not depend on the filler fraction which is opposite to what is observed in the direct comparison of a binder and a propellant. However, T_{2l} depends on the FBBA.

Both the binder 2 and the propellant 'Ref' exhibit a fraction of material relaxing at short times T_{2s}. As a consequence, this time does not correspond to the protons close to the fillers only. Notwithstanding, the protons close to the fillers have a significantly reduced mobility, notably because of the action of FBBA. This explains the decrease of the time T_{2s} as an average when fillers are introduced into the material and when the filler fraction increases.

Although the plasticizer content of the propellant 'Ref' is higher than the one of the plasticized binder, the time T_{2l} of the propellant is still shorter. Studying a filled PDMS elastomer, Litvinov and Zhdanov [15] suggested that the topological constraint, created by fillers, limits the movements of the chains. Therefore, the introduction of fillers results in a decrease of all relaxation times in the material.

Although the filler fraction has no effect on the model obtained for T_{2l}, this is the only model taking into account the influence of the FBBA. The interaction between the filler fraction and the presence of FBBA makes it difficult to distinguish their specific influence. As discussed previously [6], the FBBA creates a rigid layer of polymer around the fillers that increases the effective filler

Table 2
R^2_{adj} for the models obtained via the DoE.

Parameter p	$R^2_{adj}(p)$	$R^2_{adj}(\partial p_{,\lambda^*})$
f_s	0.83	0.30
f_m	0.79	0.64
f_l	0.97	0.77
T_{2s}	0.67	0.80
T_{2m}	0.85	0.49
T_{2l}	0.84	0.73

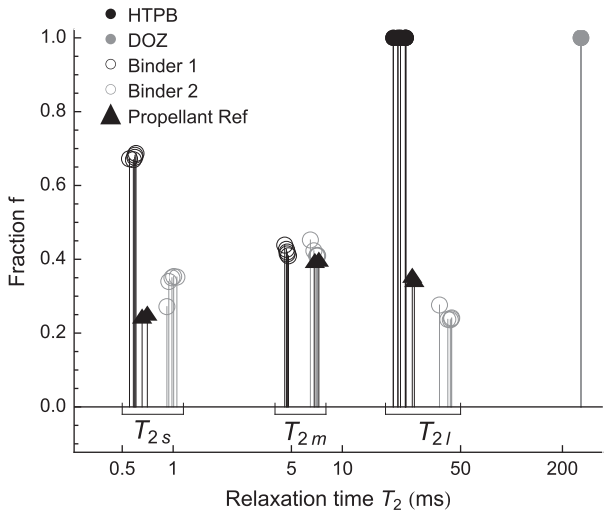

Fig. 5. Comparison of the relaxation times of the molecules, the binders, and the propellant 'Ref'.

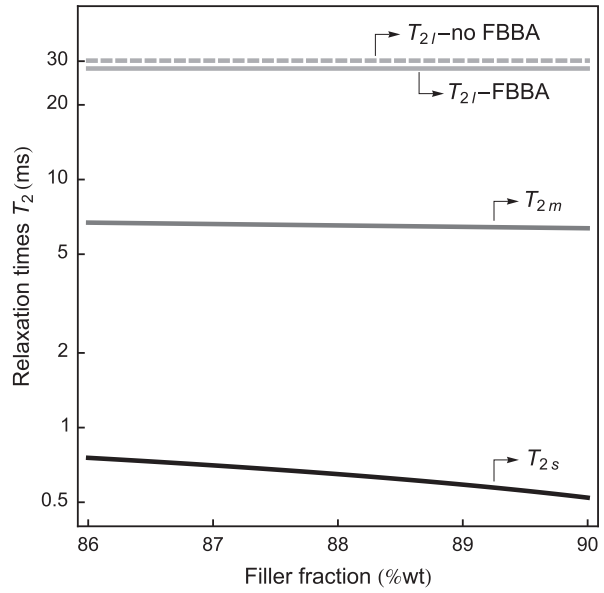

Fig. 6. Influence of the filler fraction and the FBBA on the relaxation times T_2 (NCO/OH = 0.95, plasticizer content = 20%wt of the binder).

volume, and hence the influence of the filler fraction on the studied property. In this case, the presence of FBBA decreases significantly T_{2l}, hence reducing the mobility of the less constrained segments.

3.2.2. The polymer network

Comparing HTPB chains and the binder 1 (Fig. 5), the creation of a network reduces the unique relaxation time of the free HTPB chains. Noticeably, an unfilled polymer network presents two relaxation times different by one order of magnitude and corresponding to T_{2s} and T_{2m}. Moreover, f_l decreases and f_s increases with an increase in NCO/OH ratio, while f_m remains constant (Fig. 7(a)). The constance of f_m results more likely from the shift in mobilities of chain fragments from f_l to f_m and from f_m to f_s than from the fact that the change in NCO/OH ratio does not affect the protons of f_m. Finally, all the relaxation times T_2 decrease when NCO/OH ratio increases (Fig. 7(b)).

The results prove that the various segments of the network do not exhibit an identical mobility: the constraint is larger on the protons close to a cross-link than on the ones situated further away. As a consequence, the short times T_{2s} correspond to protons on segments close to the cross-links and f_s increases with an increasing NCO/OH ratio.

Under the assumption that f_m remains constant due to the transfer of protons from f_l to f_m and from f_m to f_s, f_m corresponds to the protons of chains constrained by a cross-link but on segments situated further away from the cross-links than the protons of f_s. These segments can be located in the network or in the high molar mass sol polymer fraction that appears at high NCO/OH ratios [1].

An increase in NCO/OH ratio decreases the sol polymer fraction [1] and the fraction of material f_l corresponding to long relaxation times (Fig. 7(b)). Protons of small free polymer chains are then logically attributed to f_l. The decrease of T_{2l} with increasing NCO/OH ratio shows that the relaxation of sol polymer chains that are not directly constrained by a cross-link is still disturbed by an increase in cross-link density. The segmental mobility of the free molecules is then assumed to depend on the mesh size.

3.2.3. The sol fraction

Plasticizer molecules are by definition low molar mass molecules, contrary to polymer macromolecules. The mobility of plasticizers and the associated relaxation time T_2 are high. Indeed, the measured relaxation time for plasticizer molecules is 257 ms (Fig. 5). Thus, the relaxation of the protons of the plasticizer is identified with the third exponential term of Eq. (2) only, *i.e.* $f_l e^{-t/T_{2l}}$.

Comparing the relaxation times T_2 for the plasticizer molecules, the binder 2, and the propellant 'Ref' shows a decrease of about 150 ms in the times T_{2l} (Fig. 5). A simple averaging of the relaxation times in the f_l fraction cannot justify such a decrease. As a result, the mobility of plasticizer molecules is diminished by the neighboring polymer macromolecules; namely the polymer chains have an anti-plasticizer effect on the plasticizer. This decrease of plasticizer mobility has been observed for various filled elastomers [44] and proves that their is a physical interaction between the plasticizer molecules and the polymer chains.

The change in plasticizer content artificially influences the distribution of protons. An increase in plasticizer content increases the fraction f_l attributed to mobile segments. Since the measured quantity of material is normalized, the fractions f_s and f_m necessarily decrease. As a consequence, the influence of the plasticizer content on the fractions f is not studied.

Fig. 7(b) shows that the increase of the plasticizer content does not influence T_{2s} but increases T_{2m} and T_{2l}.

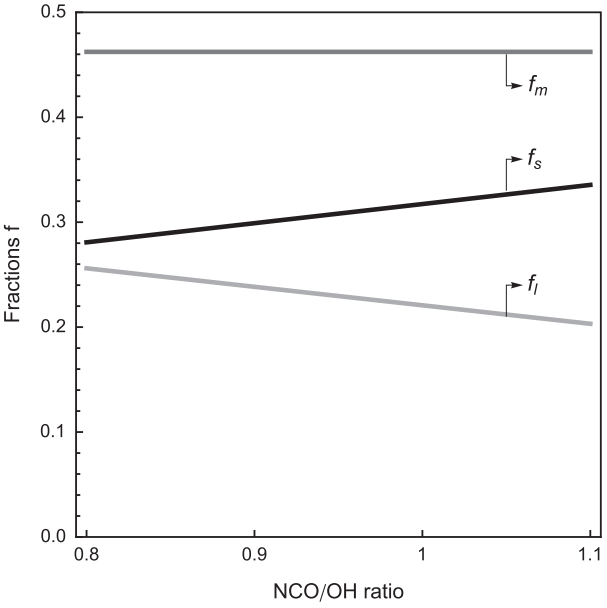

(a) Fractions f (plasticizer = 20%wt of the binder)

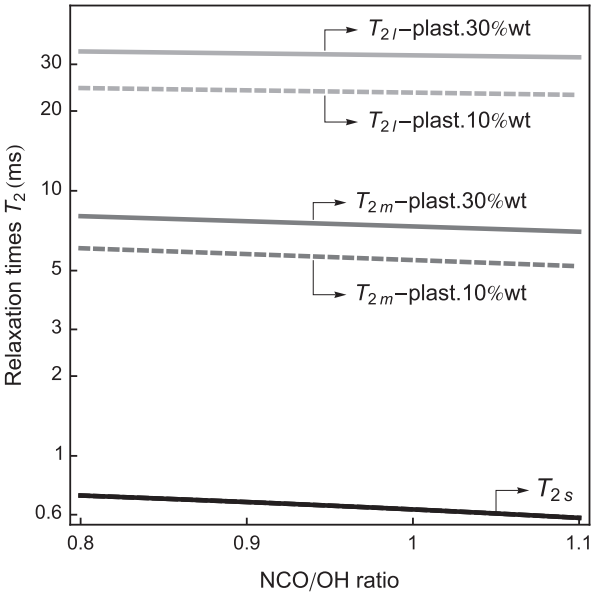

(b) Times T_2

Fig. 7. Influence of the NCO/OH ratio and the plasticizer content on the relaxation (filler fraction = 88%wt, FBBA no influence, plasticizer content in %wt of the binder).

The increase is particularly important for T_{2l}. Again, since an increase in plasticizer content increases the fraction f_l only, it also increases T_{2l} averaged over the material. This averaging effect on T_{2l} cannot be distinguished from the increase of the mobility of polymer chains due to an actual plasticizing effect. On the contrary, the increase in T_{2m} is the direct result of the increase of the mobility of the polymer segments by plasticizing.

As a conclusion, the evolution of the relaxation times according to the plasticizer content indicates an increase of the mobility of protons on polymer segments that are not directly linked to a filler surface or a cross-link.

To summarize, the measurements allow for the determination of the location of the relaxation times into the microstructure (Fig. 8). Three types of segments with distinct relaxation times are observed:

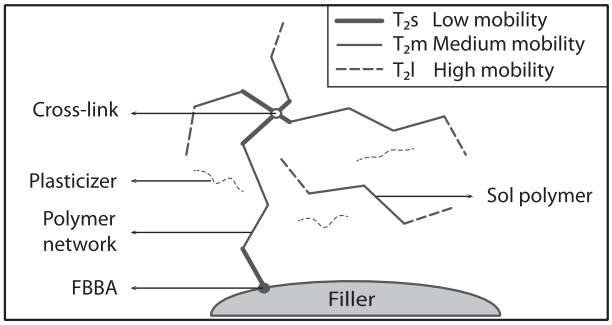

Fig. 8. Scheme of the distribution of relaxation times T_2 in the microstructure.

- f_s corresponds to the protons of the segments close to the filler surface or to a cross-link.
- f_m corresponds to the protons of the segments of the polymer chain not directly linked to a cross-link. These segments can be located in the network or the sol fraction.
- f_l corresponds to the protons of the plasticizer molecules and segments of the low molar mass sol polymer. Protons from dangling ends are also attributed to long relaxation times T_{2l}.

3.3. Micromechanisms during deformation

$\partial f_{s,\lambda^*}$ is positive whereas $\partial f_{m,\lambda^*}$ is negative over the whole studied range (Figs. 9 and 10). Moreover, $\partial f_{l,\lambda^*}$ is positive at low filler fractions and negative otherwise. $\partial f_{l,\lambda^*}$ decreases towards the negative values when FBBA are introduced.

The fraction of low mobility protons increases, while the fractions of medium and high mobility protons decrease. Therefore, stretching the material leads to at least two phenomena: a transfer of protons from f_m to f_s and a transfer of protons from f_l to f_m. Under particular conditions, a third mechanism appears: a transfer of protons from f_s or f_m to f_l.

$\partial T_{2s,\lambda^*}$ is negative and $\partial T_{2l,\lambda^*}$ is positive over the tested range. However, as the time T_{2s} decreases, the limit of measurement of the apparatus is reached and the measurement is deemed unreliable. $\partial T_{2m,\lambda^*}$ is close to zero and is positive or negative according to the levels of the filler fraction, the NCO/OH ratio, and the presence or absence of FBBA.

The average mobility T_{2s} of the protons in f_s logically decreases when the material is stretched. On the contrary, the average time T_{2l} of the protons in f_l increases with strain. Indeed, the application of the mechanical strain constrains most of the protons in the material, including part of the protons in f_l. If those protons were still contributing to f_l after stretching, T_{2l} would decrease. We assume that these protons are transferred from f_l to f_m. Only the protons able to accommodate the deformation are contributing to f_l after stretching. They belong to highly mobile molecules such as the plasticizers or the low molar mass sol polymer chains and present high relaxation times T_{2l}. As a consequence, the average time T_{2l} increases with strain.

To determine what mechanism corresponds to the observed transfer of protons from one mobility to another, we detail the influence of each factor on $\partial f_{,\lambda^*}$ and $\partial T_{2,\lambda^*}$.

3.3.1. Transfer from f_m to f_s

The filler fraction is the most influential factor on $\partial f_{,\lambda^*}$. $\partial f_{s,\lambda^*}$ increases strongly with the filler fraction while the negative $\partial f_{l,\lambda^*}$ and $\partial f_{m,\lambda^*}$ decrease strongly when the filler fraction increases. Moreover, $\partial f_{l,\lambda^*}$ and $\partial f_{m,\lambda^*}$ decrease with an increasing NCO/OH ratio. Finally, the negative $\partial T_{2m,\lambda^*}$ decreases strongly when the NCO/OH ratio increases.

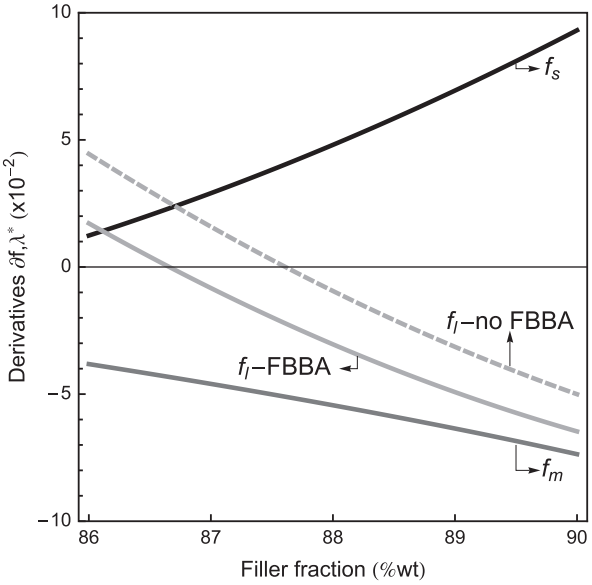

(a) Influence of mechanical strain on the fractions, $\partial f_{,\lambda^*}$

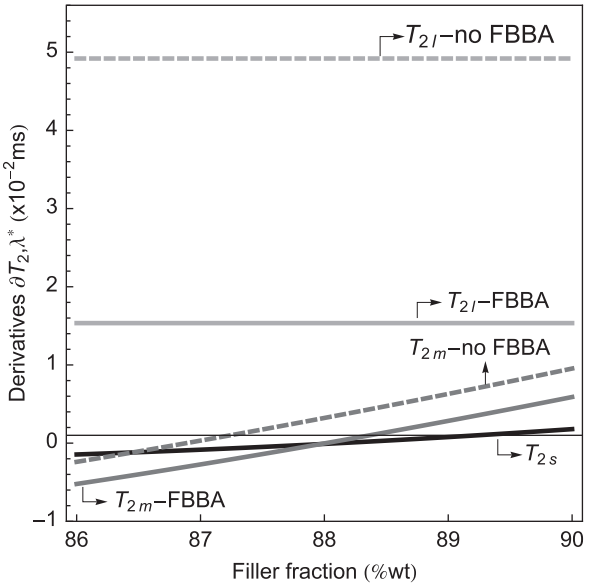

(b) Influence of the mechanical strain on the times, $\partial T_{2,\lambda^*}$

Fig. 9. Influence of the filler fraction and the FBBA on the evolution of the relaxation with mechanical strain (NCO/OH = 0.95, plasticizer content = 20%wt of the binder).

First, the rise of the filler fraction leads to a phenomenon known as strain amplification [45], which denotes that the local strain in the binder is higher than the imposed macroscopic strain and arises when rigid fillers are introduced in the binder.

Second, the fillers rearrange with the deformation and constrain the binder. The heterogeneous distribution of stresses in the microstructure leads to parts of the binder being highly stretched while others are compressed in between fillers [46,47]. Depending on the NCO/OH ratio, the network reaches its finite extensibility for a specific local strain. When the NCO/OH ratio increases, the cross-link density increases and the finite extensibility of the network decreases. Segments of the polymer network, previously attributed to f_m, become less mobile. Their relaxation time T_{2m} decreases until they transfer to f_s.

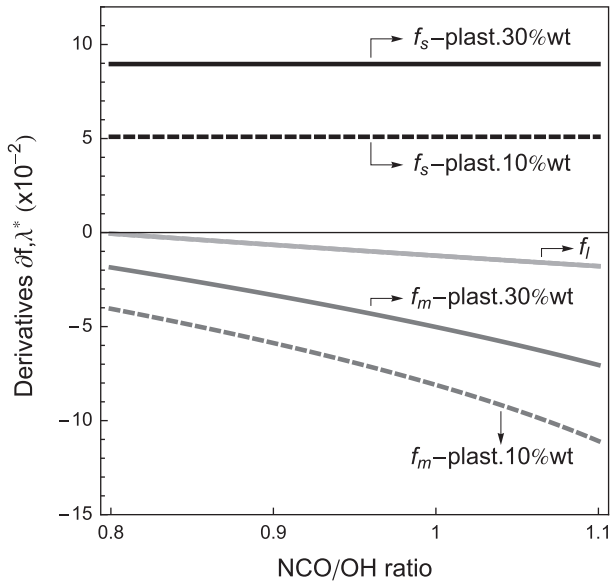

(a) Influence of mechanical strain on the fractions, $\partial f_{,\lambda*}$

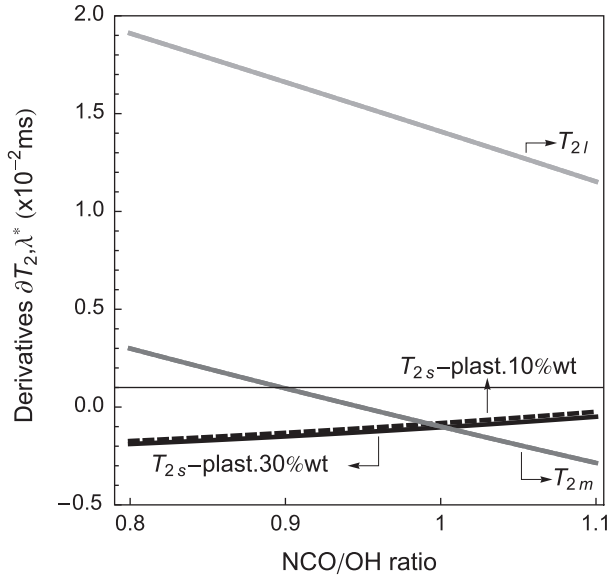

(b) Influence of the mechanical strain on the times, $\partial T_{2,\lambda*}$

Fig. 10. Influence of the NCO/OH ratio and the plasticizer content on the evolution of the relaxation with mechanical strain (filler fraction = 88%wt, no FBBA, plasticizer content in %wt of the binder).

3.3.2. Transfer from f_l to f_m

When the filler fraction increases, $\partial f_{l,\lambda^*}$ becomes negative and $\partial T_{2m,\lambda^*}$ becomes positive. An increase in the NCO/OH ratio or the introduction of FBBA decrease $\partial T_{2l,\lambda^*}$.

The increase in NCO/OH leads to a decrease of the network mesh size [1] and hence a decrease in the volume available to the high mobility protons of the free molecules or dangling ends. When the filler fraction is high, the volume taken up by the fillers is large. The presence of FBBA increases the filler effective volume and the concentration of cross-links in the vicinity of the fillers [6]. Consequently, protons attributed to f_l are constrained in the stretched polymer network, their relaxation time T_{2l} decreases until they transfer to the fraction f_m. In turn, the average measured T_{2m} increases. This phenomenon also explains the weakness of $\partial T_{2m,\lambda^*}$.

3.3.3. Increase in f_l

$\partial f_{l,\lambda^*}$ is positive when the filler fraction is small and is decreased towards the negative values by the introduction of FBBA. In addition, $\partial T_{2l,\lambda^*}$ decreases when FBBA are added. The increase of f_l with deformation implies a different mechanism, involving the removal rather than the creation of constraints.

At a low filler fraction, the volume available to the network and the sol fraction is high. In addition, the distance between fillers is increased. Finally, the influence of the FBBA on this particular effect shows that the mechanism is located at the interface between the fillers and the binder.

Two mechanisms are envisioned. First, the rupture of weak filler–binder links [48] with deformation creates dangling ends and/or sol polymer molecules. As a consequence, protons from f_s are transferred into f_m or directly into f_l.

Second, Dannenberg et al. [49] suggested that the polymer chains slide on the filler surface to accommodate deformation. This molecular rearrangements diminish internal constraints, distribute the stresses more homogeneously, and prevents the local decrease of network mesh size by stretching. The mechanism liberates sol polymer molecules that were constrained in the network either by topological or physical constraints. Therefore, protons from f_m are transferred to f_l.

4. Conclusion

The objective of this article is to identify the deformation mechanisms of a solid propellant by measuring the change in segmental mobility with deformation. The novelty lies in the investigation of the spin–spin relaxation times T_2 of a HTPB-based solid propellant by comparing isolated components, unfilled binders, and a series of solid propellants varying in composition according to a DoE.

The first result reveals that the protons in a solid propellant can be schematically divided into three segmental mobilities corresponding to three distinct relaxation times. The short times correspond to the highly restricted segments situated around cross-links or fillers. The intermediate relaxation times correspond to segments of polymer chains linked at both ends, participating to the polymer network or to the sol fraction. Finally, the long relaxation times correspond to the highly mobile segments of polymers (dangling ends) and to the plasticizer molecules.

The influence of the deformation is determined via a specific setup where the loading of the tensile machine is transmitted to the sample inside the NMR apparatus. The influence of the factors of the DoE is less visible on the derivatives of the parameters with respect to strain than on the original parameters. However, the evolution of the fraction of material corresponding to each mobility (short, medium, and long times) as well as the evolution of the relaxation times with strain suggest four mechanisms:

- The polymer network is strained in between the fillers, creating high stress bands in the microstructure and allowing the polymer chains to reach their finite extensibility. Thus, the segments of the polymer chains of the network show a decreased mobility.
- Part of the polymer in the sol fraction is immobilized in the stretched network and between fillers that are rearranging according to the imposed strain.
- In the absence of FBBA, chain sliding on the filler surface is envisioned to allow for a molecular rearrangement of the network, which leads to a more homogeneous distribution of the stress and can remove constraints on segments.

– Finally, the imposed strain might break weak filler–binder links and create dangling chains. This mechanism would also remove constraints on specific segments.

Although the presence of plasticizers limited the analysis of the highly mobile fraction, this study demonstrates the potential of the ^{1}H NMR technique to study the complex microstructure of solid propellants. Future analyses and experiments on this problem should include a more detailed comparison of binders and propellants without plasticizers in order to specify the interaction between sol and network polymer chains.

Acknowledgements

The work of AA is financially supported by DGA, Délégation Générale pour l'Armement (France). The authors would like to thank Mrs. Amiet (DGA) for supporting this project.

References

[1] Azoug A, Neviere R, Pradeilles-Duval R, Constantinescu A. Influence of cross-linking and plasticizing on the viscoelasticity of highly filled elastomers. J Appl Polym Sci 2014;131:40392.
[2] Azoug A, Neviere R, Pradeilles-Duval R, Constantinescu A. Molecular origin of the influence of the temperature on the loss factor of a solid propellant. Propellant Explos Pyrotech; submitted for publication.
[3] Azoug A, Constantinescu A, Pradeilles-Duval R, Vallat M, Neviere R, Haidar B. Effect of the sol fraction and hydrostatic deformation on the viscoelastic behavior of prestrained highly filled elastomers. J Appl Polym Sci 2013;127:1772–80.
[4] Thorin A, Azoug A, Constantinescu A. Influence of prestrain on mechanical properties of highly-filled elastomers: Measurements and modeling. Polym Test 2012;31:978–86.
[5] Azoug A, Thorin A, Neviere R, Pradeilles-Duval R, Constantinescu A. Influence of orthogonal prestrain on the viscoelastic behaviour of highly-filled elastomers. Polym Test 2013;32:375–84.
[6] Azoug A, Neviere R, Pradeilles-Duval R, Constantinescu A. Influence of fillers and bonding agents on the viscoelasticity of highly filled elastomers. J Appl Polym Sci 2014;131:40664.
[7] Mowery D, Assink R, Celina M. Sensitivity of proton NMR relaxation times in a HTPB based polyurethane elastomer to thermo-oxidative aging. Polymer 2005;46:10919–24.
[8] Kinsey R. Solid-state NMR of elastomers. Rubber Chem Technol 1990; 63:407–25.
[9] Cosgrove T, Griffiths P. Nuclear magnetic resonance studies of adsorbed polymer layers. Adv Colloid Interface Sci 1992;42:175–204.
[10] Litvinov V, Steeman P. EPDM-carbon black interactions and the reinforcement mechanisms, as studied by low-resolution ^{1}H NMR. Macromolecules 1999;32:8476–90.
[11] Sun X, Isayev A, Joshi T, von Meerwall E. Molecular mobility of unfilled and carbon-black-filled isoprene rubber: proton NMR transverse relaxation and diffusion. Rubber Chem Technol 2007;80:854–72.
[12] Kaufman S, Slichter W, Davis D. Nuclear magnetic resonance study of rubber–carbon black interactions. J Polym Sci Part A-2 1971;9:829–39.
[13] Nishi T. Effect of solvent and carbon species on the rubber–carbon black interactions studied by pulsed NMR. J Polym Sci: Polym Phys 1974;12:685–93.
[14] Litvinov V. Molecular-dynamic processes on the polydimethylsiloxane-filler interface. Polym Sci USSR 1988;30:2250–6.
[15] Litvinov V, Zhdanov A. Role of various factors in the restriction of molecular mobility of polymer chains in filled polymers. Polym Sci USSR 1988; 30:1000–6.
[16] Berriot J, Martin F, Montes H, Monnerie L, Sotta P. Reinforcement of model filled elastomers: characterization of the cross-linking density at the filler–elastomer interface by ^{1}H NMR measurements. Polymer 2003;44:1437–47.
[17] Shim S, Isayev I, von Meerwall E. Molecular mobility of ultrasonically devulcanized silica-filled poly(dimethylsiloxane). J Polym Sci Polym Phys 2003;41:454–65.
[18] Litvinov V, Orza R, Kluppel M, Van Duin M, Magusin P, et al. Rubber–filler interactions and network structure in relation to stress–strain behavior of vulcanized, carbon black filled EPDM. Macromolecules 2011;44:4887–900.
[19] McBrierty V, Kenny J. Structural investigations of carbon black-filled elastomers using NMR and ESR. Kautsch Gummi Kunstst 1994;47:342–8.
[20] Dreiss C, Cosgrove T, Benton N, Kilburn D, Alam M, Schmidt R, et al. Effect of crosslinking on the mobility of PDMS filled with polysilicate nanoparticles: positron lifetime, rheology and NMR relaxation studies. Polymer 2007; 48:4419–28.
[21] Deloche B, Samulski E. Short-range nematic-like orientational order in strained elastomers: a deuterium magnetic resonance study. Macromolecules 1981; 14:575–81.
[22] Gronski W, Stadler R, Jacobi M. Evidence of nonaffine and inhomogeneous deformation of network chains in strained rubber-elastic networks by deuterium magnetic resonance. Macromolecules 1984;17:741–8.
[23] Spiess H. Deuteron NMR – a new tool for studying chain mobility and orientation in polymers. Adv Polym Sci 1985;66:23–58.
[24] Dubault A, Deloche B, Herz J. Effects of trapped entanglements on the chain ordering in strained rubbers: a deuterium magnetic resonance investigation. Macromolecules 1987;20:2096–9.
[25] Sotta P, Fülber C, Demco D, Blümich B, Spiess H. Effect of residual dipolar interactions on the NMR relaxation in cross-linked elastomers. Macromolecules 1996;29:6222–30.
[26] Callaghan P, Samulski E. Molecular ordering and the direct measurement of weak proton–proton dipolar interactions in a rubber network. Macromolecules 1997;30:113–22.
[27] Nishi T, Chikaraishi T. Pulsed NMR studies of elastomers under large deformation. J Macromol Sci-Phys 1981;B19:445–57.
[28] Cohen-Addad J, Huchot P. Vulcanized polybutadiene. Swelling and NMR observation of stretching. Macromolecules 1991;24:6591–9.
[29] Litvinov V, Spiess H. Molecular mobility in the adsorption layer and chain orientation in strained poly(dimethylsiloxane) networks by ^{2}H NMR. Makromol Chem 1992;193:1181–94.
[30] Hailu K, Fechete R, Demco D, Blümich B. Segmental anisotropy in strained elastomers detected with a portable NMR scanner. Solid State Nucl Mag 2002; 22:327–43.
[31] Hedesiu C, Demco D, Remerie K, Blümich B, Litvinov V. Study of uniaxially stretched isotactic poly(propylene) by ^{1}H solid-state NMR and IR spectroscopy. Macromol Chem Phys 2008;209:734–45.
[32] Sotta P, Deloche B, Herz J, Lapp A, Durand D, Rabadeux J. Evidence of short-range orientational couplings between chain segments in strained rubbers: a deuterium magnetic resonance investigation. Macromolecules 1987; 20:2769–74.
[33] Sotta P, Deloche B. Uniaxiality induced in a strained poly(dimethylsiloxane) network. Macromolecules 1990;23:1999–2007.
[34] Valić S, Judeinstein P, Deloche B. Analysis of deuterium NMR spectra of probe chains diffusing in a stretched polybutadiene network. Polymer 2003;44:5263–7.
[35] Davenas A, Chap. X Les propergols composites. In: Davenas A, editor. Technologie des propergols solides, Masson, Paris Milan Barcelone Mexico; 1989. p. 461–10.
[36] Carr H, Purcell E. Effects of diffusion on free precession in nuclear magnetic resonance experiments. Phys Rev 1954;94:630–8.
[37] Meiboom S, Gill D. Modified spin-echo method for measuring nuclear relaxation times. Rev Sci Instrum 1958;29:688–91.
[38] Horch C, Schlayer S, Stallmach F. High-pressure low-field ^{1}H NMR relaxometry in nanoporous materials. J Magn Reson 2014;240:24–33.
[39] Hansen M, Boeffel C, Spiess H. Phenylene motion in polycarbonate: influence of tensile stress and chemical modification. Colloid Polym Sci 1993; 271:446–53.
[40] Litvinov V. Strain-induced phenomena in amorphous and semicrystalline elastomers. Solid state ^{1}H NMR T_2 relaxation under uniaxial compression. Macromolecules 2001;34:8468–74.
[41] Böhme U, Gelfert K, Scheler U. Solid state NMR on polymers under mechanical stress. In: Magnetic resonance in porous media, AIP Conference proceedings; 2011. p. 109–12.
[42] Treloar L. The elasticity and related properties of rubbers. Rubber Chem Technol 1974;47:625–96.
[43] Ezekiel M. The application of the theory of error to multiple and curvilinear correlation. J Am Statist Assoc 1929;24(165A):99–104.
[44] Litvinov V. EPDM/PP thermoplastic vulcanizates as studied by proton NMR relaxation: phase composition, molecular mobility, network structure in the rubbery phase, and network heterogeneity. Macromolecules 2006; 39:8727–41.
[45] Mullins L, Tobin N. Stress softening in rubber vulcanizates. Part I. Use of a strain amplification factor to describe the elastic behavior of filler-reinforced vulcanized rubber. J Appl Polym Sci 1965;9:2993–3009.
[46] Azoug A. Micromécanismes et comportement macroscopique d'un élastomère fortement chargé, PhD thesis, Ecole Polytechnique; 2010.
[47] Matous K, Inglis H, Gu X, Rypl D, Jackson T, Geubelle P. Multiscale modeling of solid propellants: from particle packing to failure. Compos Sci Technol 2007; 67:1694–708.
[48] Bueche F. Molecular basis for the Mullins effect. J Appl Polym Sci 1960; 4:107–14.
[49] Dannenberg E, Brennan J. Strain energy criterion for stress softening in carbon black-filled vulcanizates. Rubber Chem Technol 1966;39:597.